

Inhibition of Corrosion of Pure Iron by Quaternized Poly(4-Vinylpyridine)-Graft-Bromodecane in Sulphuric Acid

A. Chetouani^{1,2}, K. Medjahed³, S.S. Al-Deyab⁴, B. Hammouti^{1,*}, I. Warad⁴, A. Mansri³, A. Aouniti¹

¹ LCAE-URAC18, Faculté des Sciences, Université Mohammed Premier, Oujda, Morocco.

² Laboratoire de chimie physique, Centre Régionale des Professions de l'Éducation et de Formation "CRPEF", Académie Régionale de l'Orientale, Oujda, Morocco.

³ Laboratoire d'Application des Electrolytes et des Polyelectrolytes Organiques (LAEPO), Département de Chimie, Université de Tlemcen, BP 119, 13000 Tlemcen, Algeria

⁴ Petrochemical Research Chair, Department of Chemistry, College of Science, King Saud University, B.O. 2455, Riadh 11451, Saudi Arabia

*E-mail: hammoutib@gmail.com

Received: 21 May 2012 / Accepted: 9 June 2012 / Published: 1 July 2012

A brief review is given to study inhibitive action of Poly (4-vinylpyridine) – Graft - Bromodecane (P4VPBrD) at three degrees of quaternisation (25%, 45% and 60 %) on the corrosion behaviour of pure iron was investigated in deaerated molar sulphuric acid solution using weight loss measurements, potentiodynamic polarisation, and impedance spectroscopy (EIS) methods at free corrosion potential. A polarisation measurement shows also that the compound acts as a mixed-type inhibitor and was adsorbed on the iron surface according to the Langmuir adsorption isotherm model. The parameters, which characterise the corrosion behaviour, can be determined from plots and diagrams of Nyquist. Their inhibition efficiency (E %) increases with the all inhibitors concentration. Trends in the increase of charge transfer resistance and decrease of capacitance values also shows the molecular adsorption on the metal surface. The temperature effect on the corrosion, behaviour iron metal in 1M H₂SO₄ without and with inhibitor at 510⁻⁵M was studied at the temperature range from 298 to 338 K, the associated activation energy have been determined and proved that the adsorption is a spontaneous process.

Keywords: Iron, poly (4-vinylpyridine), inhibition, corrosion, Sulphuric acid.

1. INTRODUCTION

Iron products are used in almost all industrial sectors of the economy. The cost of corrosion has been reported from many studies to be in order of 1 to 5 percent of GNP for any country. Corrosion

never stops but its scope and severity can be lessened. In a sense, using inhibitors is one of best-known methods of corrosion protection [1-3]. The importance of inhibitive protection in acidic solutions is increased by the fact that iron materials which are more susceptible to be attacked in aggressive media, are the commonly exposed metals in industrial environments

The anticorrosive protective properties of these inhibitors are determined by a complex mechanism which include action of different factors [4-9]: (a) the adhesion of inhibitor to the substrate, (b) the water, oxygen and ionic inhibitor uptake; (c) the inhibitor formulation; (d) inhibitor concentration; (e) chemical composition and surface pre-treatment of the metallic surface; (f) environmental conditions; and (g) electrochemical corrosion reactions at the metal/solution interface. The protective properties of organic inhibitor can be attributed also to a barrier and to an electrochemical mechanism. Generally, organic coatings have a high resistance to ionic conductivity; they offer good barrier properties retarding diffusion chemical species to and from metal surface. Organic compounds were interested as corrosion inhibitors in acid pickling baths [10-13].

The selection of such inhibitor at given system depends in its inherent stability versus the corrosion medium, the metal nature, the charge magnitude at metal-solution interface and cathode reaction. The compounds used as inhibitors act through a process of surface adsorption, so the efficiency of inhibitor depends not only on environment characteristics in which its acts, the metal nature surface and electrochemical potential at interface, but also on the inhibitor structure itself, which includes adsorption active centres number in molecular, there charge density, size molecule, adsorption mode, metallic complex formation and inhibitor projected area on metallic surface [14-16]. Inhibitors adsorption at metal/solution interface was usually accepted as electrostatic formation or covalent bonding between metal surface atoms and adsorbents [4, 5, 8, 14, 17-23].

The application water-soluble polymers as corrosion inhibitors of metals in aggressive media, takes recently more attention. The inhibitive polymers power was related structurally with various active centres adsorption such as cyclic rings and heteroatom's as oxygen, nitrogen and sulphur, which are major active centres adsorption. PVP and derivates, polyvinyl pyridine, polyvinylbipyridine, polyvinylpyrrolidone (PVP), polyethylenimine (PEI) and polyvinylimidazoles (PVI) has been widely examined, has received particular attention and has been applied to inhibition of Fe, Cu, Al, Zn and there alloys in various acidic media [24-32].

Recently, the encouragement result obtained by addition of poly (4-vinylpyridine) (P4VP) derivatives on the corrosion of pure iron in 1M H₂SO₄ has incited us to modify molecular structure by introducing poly-3-oxide ethylene group [33-35]. P4VP and its derivatives, the poly (4-vinylpyridine poly-3-oxide ethylene) (P4VPPOE), obtained good results and Poly (4-vinylpyridine isopentyl bromide) P4VPIPBBr on the corrosion of pure iron in 1M H₂SO₄ [27, 28]. The adsorption of these molecules depends mainly on some physico-chemical properties of the inhibitor such as the functional groups, steric factors, cyclic rings, electron density at donor atoms and p-orbital character of donating electrons, and electronic structure molecular [4, 5, 14, 27, 28, 36-38].

In this work, the study was made using pure iron immersed in molar hydrochloric acid without and with addition of Poly (4-Vinylpyridine) – Graft - Bromodecane at three degree of quaternisation 25%, 45% and 60%, P4VPBrD, (Figure 1) newly synthesized, with respective average molecular

weights ($5.9 \cdot 10^5$; $7.22 \cdot 10^5$ and $9.45 \cdot 10^5$ g/mol), respectively as inhibitor for iron corrosion in 1M H_2SO_4 .

2. EXPERIMENTAL

2.1. Inhibitors

Poly (4-vinylpyridine) (P4VP) is prepared by radical polymerization of 4-vinylpyridine in methanol, under vacuum, with azobisisobutyronitrile (AIBN) as initiator, as described elsewhere [27, 28]. The polymerization fractionated by partial precipitation from methanol solution with ethyl petrol. Poly (4-Vinylpyridine) - Graft-Bromodecane P4VPBrD is obtained by mixing P4VP to Bromodecane (BrD) in chloroform (CH_3Cl) in a thermostatic bath ($70^\circ C$). P4VPBrD is obtained then precipitated in petrol ether, washed in ethanol, precipitated again in petrol ether and dried. The structure is checked by NMR and IR spectra. The molecular weight is estimated by the viscosity technique using ethanol as solvent [27, 28, 39]. P4VPBrD is obtained in three degrees of quaternisation (25, 45 and 60%). P4VPBrD (I) at (25%), P4VPBrD (II) at (45%) and P4VPBrD (III) at (60%) are obtained after 24, 120 and 240 h, respectively. The Poly (4-Vinylpyridine) - Graft-Bromodecane molecular structure of newly synthesized P4VBrD is shown in schema 1.

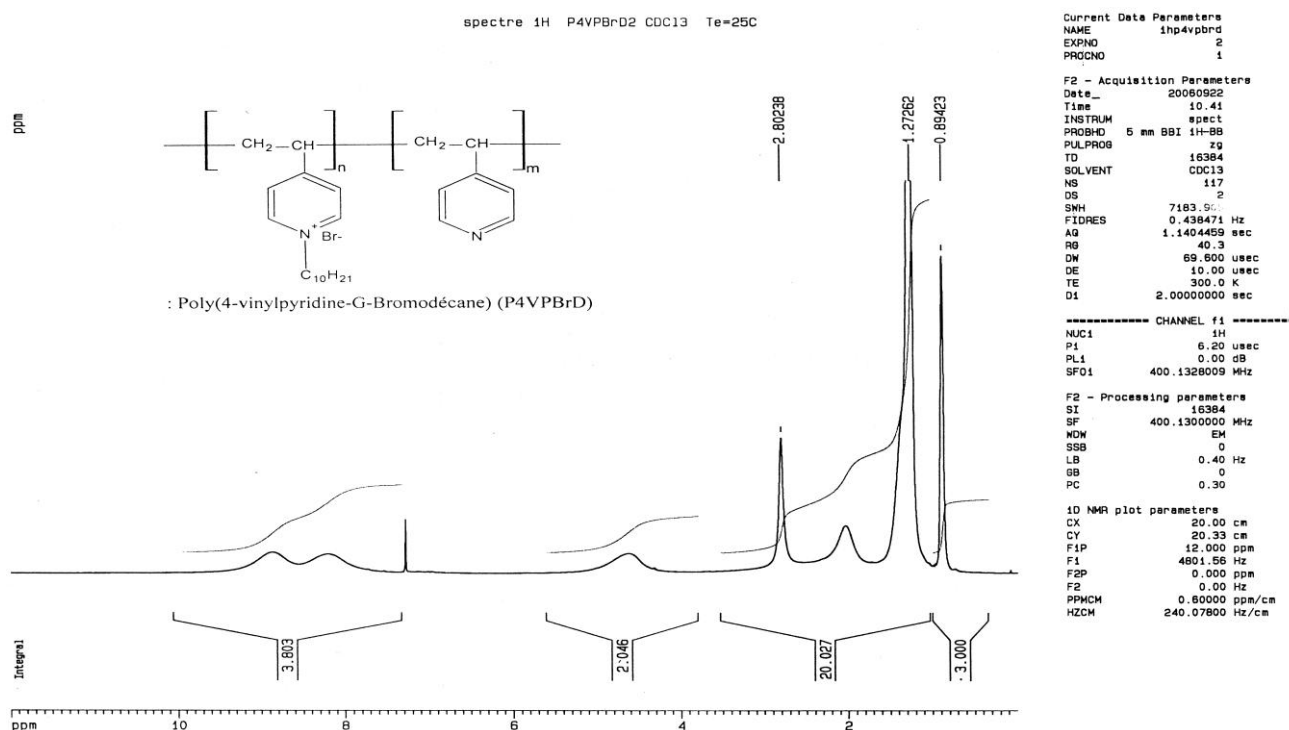
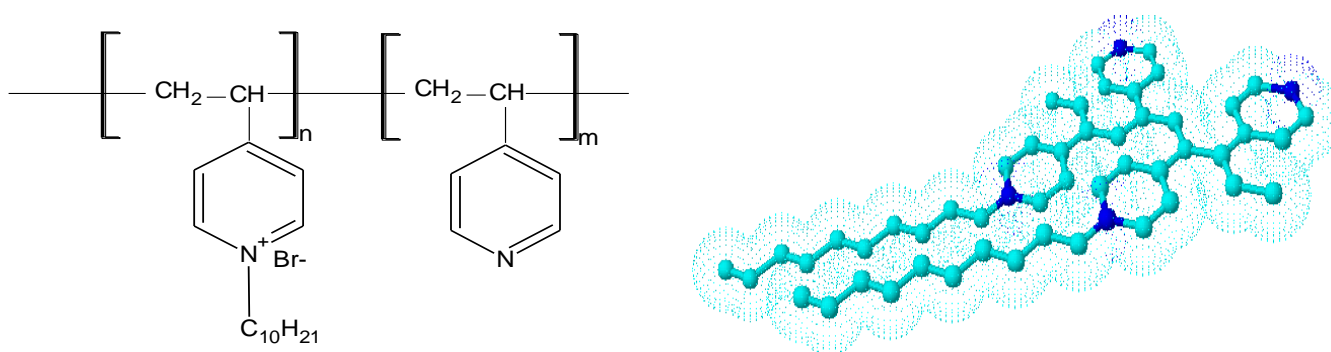


Figure 1. 1H NMR spectra of P4VPBrD copolymer in D_2O/DCl as solvent

These polymer are analysed are characterised by Proton nuclear magnetic resonance (1H NMR) with a DMX-500 (Bruker Company, Germany) and the solvents were D_2O/DCl . figure 1. UV-Visible absorption spectra were recorded with Shimadzu UV 260 spectrometer. The molecular weight was determined by water size exclusion chromatography (GPC) using a set of three columns TSK PWXL

obtained from TOSO Haas (length $\frac{1}{4}$ 30 cm, interior diameter $\frac{1}{4}$ 7.8 cm) and coupled to an automatic refractometer or light scattering apparatus. The viscosity technique was using (Ubbelohde viscometer) to determined molecular weight, with a thermostated bath at $25 \pm 0.1^\circ\text{C}$. The molecular weight is estimated using ethanol as solvent. Poly (4-Vinylpyridine) - Graft-Bromodecane, three degree of quaternisation 25%, 45% and 60% of average molecular weight $5.9 \cdot 10^5$; $7.22 \cdot 10^5$; 9.4510^5 g/mol, respectively, were obtained as inhibitor application for iron corrosion in 1M H_2SO_4

The figure 1 shows the characterization ^1H NMR spectra of (P4VPBrD). The peaks at $\delta = 8.92$ (ppm) and at $\delta = 8.32$ are ascribed to the protons at the 2, 6 sites and 3, 5 sites of the pyridine ring respectively. Comparing the ^1H NMR of (P4VPBrD) with that of the polymer P4VP; a new peak at $\delta = 2.80$ is assigned to the eighteen protons and $\delta = 0.89$ to methyl of group bonded with N atom in the pyridine ring. The ratio of peak areas of the above four peaks ($\delta = 8.92, 8.32, 2.80$ and 0.89) which is equal to the number of the protons in the corresponding groups in (P4VPBrD).



Scheme 1. The molecular structure of P4VPBrD.

2.2. Gravimetric, polarisation and impedance spectroscopy measurements

Prior to all measurements, the iron samples (99.5%, thickness = 0.05 cm from Good Fellow, Cambridge, England) are polished with different emery paper up to 1000 grade, washed thoroughly with bidistilled water degreased and dried with acetone. The aggressive solution (1M H_2SO_4) is prepared by dilution of Analytical Grad 98% H_2SO_4 with bidistilled water.

Weight loss was measured on sheets of pure iron of 4cm^2 apparent surface area. The iron samples are immersed in 100ml of the corrosive medium. The immersion time for the weight loss measurements was 1 hours at 298K.

Electrochemical experiments were recorded using an Amel potentiostat (model 449) at a scan rate of 20mV/min. A platinum counter electrode and a saturated calomel electrode (SCE) were used. The working electrode (WE) in the form of disc was cut from pure iron and was embedded in polytetrafluoroethylene (PTFE).

The test solution was deaerated for 30min at E_{corr} in the cell with pure nitrogen. Gas pebbling was maintained through the experiments. Before recording the cathodic polarisation curves, the iron electrode was polarised at -800 mV/SCE for 10min.

A polarisation resistance measurement is performed by scanning through a potential range which is very close to the corrosion potential. The potential range is $\pm 10\text{mV}$ around E_{corr} . The resulting current is plotted versus potential. Polarisation resistance (R_p) values are obtained from the current potential plot.

Impedance spectroscopy measurements are carried out in a conventional three electrodes electrolysis cylindrical Pyrex glass cell. The working electrode (WE) had the form of a disc cut from iron sheet. The exposed area to the corrosive solution is 1cm^2 . A saturated calomel electrode (SCE) and a disc platinum electrode are used, respectively, as a reference and auxiliary electrode. The temperature is thermostatically controlled at $298 \pm 1\text{K}$.

The electrochemical impedance spectroscopy (EIS) measurements are carried out with the electrochemical system (Tacussel), which included a digital potentiostat model Volta lab PGZ 100 computer at E_{corr} after immersion in solution without bubbling. After the determination of steady-state current at a given potential, sine wave voltage (10mV) peak to peak, at frequencies between 100kHz and 10mHz are superimposed on the rest potential. Computer programs automatically controlled the measurements performed at rest potentials after 30 min of exposure. The impedance diagrams are given in the Nyquist representation. Before recording the curves the test solution is de-aerated in magnetically stirred for 30 min in the cell with nitrogen. The method used to analyze EIS spectra is equivalent circuit modelling in our case was modelled using the zview2.8d software after converting data from Radiometer Analytical EIS file converter

3. RESULTS AND DISCUSSION

3.1. Weight loss measurements:

The effect of addition of Poly (4-Vinylpyridine) - Graft-Bromodecane at tree degree of quaternisation 25%, 45% and 60% tested at different concentrations on the corrosion of iron in 1M H_2SO_4 solution was studied by weight-loss at 298K after 1 hours of immersion period. Inhibition efficiency ($E\%$) was calculated as follows equation 1 [15, 16, 27], where W and W' are the corrosion rates of iron samples in the absence and presence of organic polymer, respectively:

$$E_w = 100 \times \left(1 - \frac{W'}{W} \right) \quad (1)$$

Table 1 collects the values of corrosion rates of iron and inhibition efficiency of Poly (4-Vinylpyridine) - Graft-Bromodecane at tree degree of quaternisation 25%, 45% and 60% compounds tested at various concentrations. According to this table and from gravimetric measurements, the results show for each compounds tested, the corrosion rate values of pure iron decrease when the concentration of Poly (4-vinylpyridine)-G-Bromodecane at tree degree of quaternisation 25%, 45% and 60% increases. The inhibiting action is more pronounced with 10^{-5}M (100%) which is the maximal concentration of polymer.

We conclude that Poly (4-Vinylpyridine) - Graft-Bromodecane at tree degree of quaternisation

25%, 45% and 60% is a best inhibitor and the inhibition efficiency attains respectively 100%, 98% and 94%. We note again, the inhibitory efficiency is independent of quaternisation degree of poly (4-vinylpyridine-isopentyl bromide). This result is at good agreement with that obtained by poly (4-vinylpyridine poly-3-oxide ethylene) at two degree of quaternisation 20% and 80% in corrosion of iron in molar sulphuric acid [33-35] and poly (4-vinylpyridine isopentyl bromide) (P4VPIBr) at three degrees of quaternisation (6%, 18% and 79 %) [28].

Table 1. Pure iron weight loss data and inhibition efficiency of P4VPBrD at tree degree of quaternisation

Inhibitors		W (mg.cm ⁻² .h ⁻¹)	Ew (%)
1M H ₂ SO ₄		2.488	-
P4VPBrD at degree of quaternisation 25%.	510 ⁻⁵	0.000	100
	10 ⁻⁵	0.000	100
	510 ⁻⁶	0.034	98.6
	10 ⁻⁶	0.134	94.6
	5.10 ⁻⁷	0.905	63.6
	10 ⁻⁷	1.175	52.8
	510 ⁻⁸	1.273	48.8
	10 ⁻⁸	1.689	32.1
P4VPBrD at degree of quaternisation 45%.	510 ⁻⁵	0.000	100
	10 ⁻⁵	0.049	98.0
	510 ⁻⁶	0.245	90.1
	10 ⁻⁶	0.249	90.0
	5.10 ⁻⁷	0.979	60.6
	10 ⁻⁷	1.126	54.7
	510 ⁻⁸	1.322	46.9
	10 ⁻⁸	1.738	30.1
P4VPBrD at degree of quaternisation 60%.	510 ⁻⁵	0.000	100
	10 ⁻⁵	0.147	94.1
	510 ⁻⁶	0.220	91.1
	10 ⁻⁶	0.274	88.9
	5.10 ⁻⁷	0.783	68.5
	10 ⁻⁷	1.192	52.1
	510 ⁻⁸	1.395	43.9
	10 ⁻⁸	1.713	31.1

3.2. Polarisation measurements:

Current-potential characteristics resulting from cathodic and anodic polarization curves of iron in normal H₂SO₄ at various concentrations of Poly (4-vinylpyridine) – Graft - Bromodecane at tree degree of quaternisation 25%, 45% and 60% inhibitors are evaluated. Figure (2) shows the typical cathodic Tafel and anodic plots of Poly (4-vinylpyridine) – Graft - Bromodecane at tree degree of

quaternisation 45% at different concentrations. Table (3) collects electrochemical parameters at various concentrations of *P4VPBrD* at tree degree of quaternisation 25%, 45% and 60% and inhibition efficiencies $E_I\%$ can be determined by the equation 2 [14, 37, 38, 40], where I_{corr}° and I_{corr} are the corrosion current density values without and with the inhibitor, respectively, determined by extrapolation of cathodic Tafel lines to corrosion potential.

$$E_I = 100 \times \left(1 - \frac{I_{corr}}{I_{corr}^\circ} \right) \tag{2}$$

The polarisation resistance (R_p) and corresponding efficiency inhibition values of pure iron in 1M H_2SO_4 in the absence and presence of different concentration of *P4VPBrD* at tree degree of quaternisation 25%, 45% and 60% are also given in Table (2). In this case the inhibition efficiency ($E_R\%$) is calculated by equation 3, where R_p and R'_p are the polarisation resistance with and without the inhibitor, respectively.

$$E_R \% = \left(1 - \frac{R_p}{R'_p} \right) \cdot 100 \tag{3}$$

From electrochemical polarisation measurements, it is clear that the addition of the polymer *P4VPBrD* at tree degree of quaternisation 25%, 45% and 60% at various concentrations leads to a decrease in the cathodic current densities table 3.

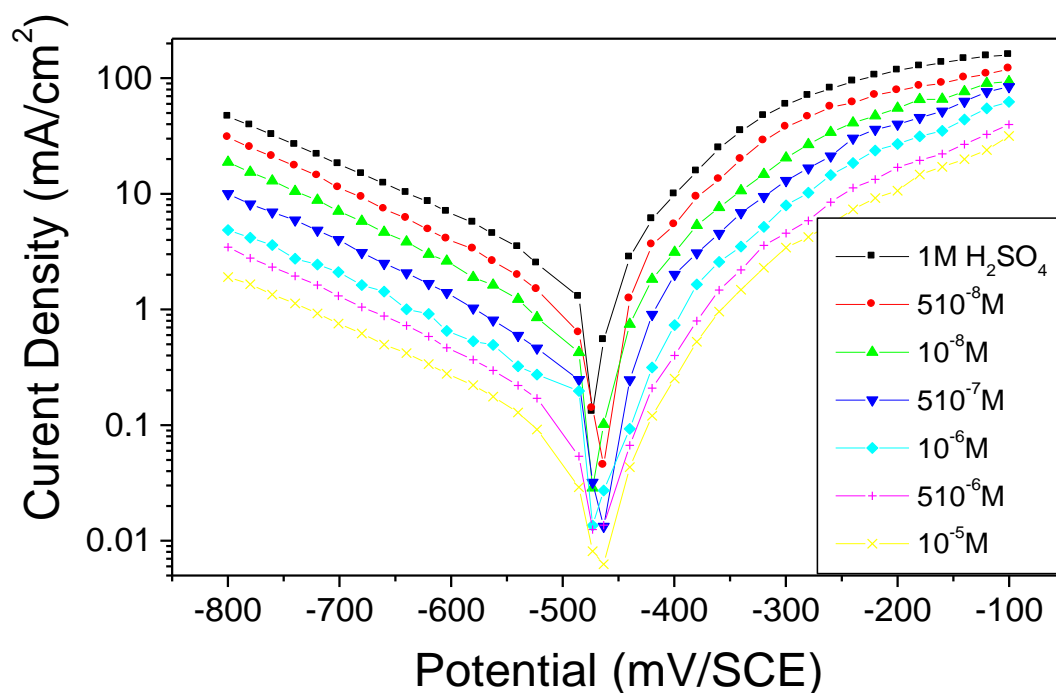


Figure 2. Polarisation plots of iron in 1M H_2SO_4 for various concentrations of *P4VPBrD* at degree of quaternisation 45%.

The cathodic portions rise to Tafel lines indicating that the hydrogen evolution reaction is control activation. The addition of the polymer to the corrosive solution does not modify the cathodic Tafel slope (b_c) and then the mechanism of the process is not affected. The free corrosion potential determined after 1 hour of immersion does not change in the presence of the inhibitor [11-14, 22, 38, 41].

These results demonstrate that the hydrogen evolution reaction is inhibited and the inhibition efficiency increases with P4VPBrD at degree of quaternisation 45% concentration to attain a maximum value of 98% at 10^{-5} M.

The anodic curves with and without P4VPBrD at degree of quaternisation 45% show that the inhibition mode depended upon electrode potential Figure (2). It seems that, the presence of the P4VPBrD studied does not change the current versus potential characteristics. This result indicates that all the tested P4VPBrD act mixed inhibitors. The observed phenomenon is generally described as corrosion inhibition of the interface associated with the formation of a protective layer of adsorbed inhibition species at the electrode surface [42-44].

Table 2. Electrochemical parameters for iron in 1M H_2SO_4 at various concentrations of P4VPBrD at degree of quaternisation 45% at 298K.

C (M)	E_{corr} (mV/SCE)	b_c (mV/dec.)	I_{corr} ($\mu A/cm^2$)	E_I (%)	R_p (Ω / cm^2)	E_R (%)
Blank	-465	235	1650	-	22	-
10^{-8}	-478	220	1221	26	31	29
10^{-7}	-476	217	907	45	43	49
$5 \cdot 10^{-7}$	-474	219	577	65	65	66
10^{-6}	-475	218	148	91	200	89
$5 \cdot 10^{-6}$	-473	222	99	94	440	95
10^{-5}	-474	223	33	98	935	98

From polarisation resistance measurements Table (2), we remark that R_p increases with increasing of P4VPBrD at degree of quaternisation 45% inhibitor concentration. $E\%$ increases with the increase of inhibitor concentration to attain 98% at 10^{-5} M. We may conclude that the inhibition efficiencies of P4VPBrD at degree of quaternisation 45% obtained by electrochemical, polarisation resistance and weight loss methods are in good agreement.

3.3 Impedance spectroscopy measurements.

Electrochemical Impedance Spectroscopy (EIS) is a powerful diagnostic tool that we can use to characterize limitations and improve the performance of systems. By applying physically-sound

equivalent circuit models wherein physiochemical processes occurring in interface electrolyte-surface are represented by a network of resistors, capacitors and inductors, we can extract meaningful qualitative and quantitative information regarding the sources of impedance within of the system.

The corrosion behaviour of iron, in acidic solution in the presence and absence of Poly (4-vinylpyridine) – Graft - Bromodecane at tree degree of quaternisation 25%, 45% and 60% compound, is investigated by the electrochemical impedance spectroscopy (EIS) at 298 K after 30 min of immersion.

The charge-transfer resistance (R_t) values are calculated from the difference in impedance at lower and higher frequencies, as suggested by Tsuru et al [45] . To obtain the double layer capacitance (C_{dl}) the frequency at which the imaginary component of the impedance is maximal ($-Z_{max}$) is found as represented in equation [14, 32, 38].

$$C_{dl} = \frac{1}{\omega R_t} \quad \text{Where } \omega = 2\pi f_{max} \quad (4)$$

The inhibition efficiency obtained from the charge transfer resistance is calculated by equation where $R_{t/inh}$ and R_t are the charge transfer-resistance values with and without inhibitor, respectively.

$$E(\%) = \frac{\left[R_{t/inh} - R_t \right]}{R_{t/inh}} \cdot 100 \quad (5)$$

Figure (3) shows a set of Nyquist impedance diagrams obtained from the pure iron electrode exposed for 30 min at the free corrosion potential in inhibited and uninhibited acidic solutions containing various concentrations of P4VPBrD at degrees of quaternisation 45%. It is seen from this figure (3) that the impedance diagrams are almost semicircular in appearance but not perfect semicircles. We deduce the centre of the semicircles does not lie on the Z_{reel} axe, but is shifted to negative Z_{im} values. This difference has been attributed to the frequency dispersion [28, 46]. The data table3 reveal that, each impedance diagram of pure iron electrode exposed for 30 min at the free corrosion potential in inhibited and uninhibited acidic solution containing at different concentrations of P4VPBrD at degrees of quaternisation 45% consists of a large capacitive loop.

The capacitive loop could be assigned to the relaxation process and its dielectric properties [47]. The effect of P4VPBrD at degrees of quaternisation 45% on the impedance response of pure iron in desaerated 1M H_2SO_4 solution at 298K is independent of degrees of quaternisation of these polymers. This loop makes an angle with the real axis and its intersection gives a value of the resistance of the solution enclosed between the working electrode and the counter electrode (R_s).

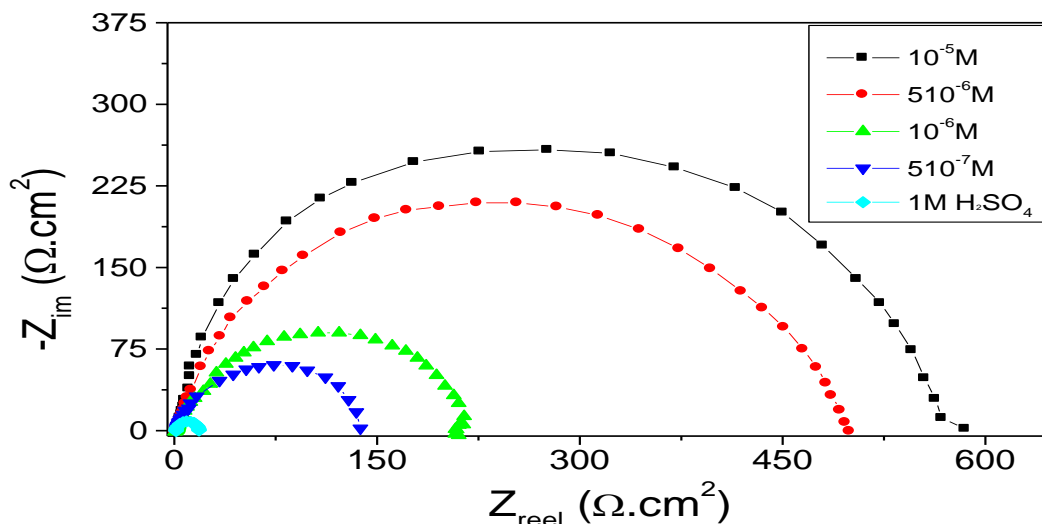


Figure 3. Impedance diagrams of iron electrode in 1M H₂SO₄ in presence and absence of P4VPBrD at degrees of quaternisation 45%.

As the impedance diagram obtained has a semicircle appearance, it shows that a charge transfer process mainly controls the corrosion of iron. It is apparent also from these figures 3, which the charge transfer-resistance value of pure iron in uninhibited H₂SO₄ solution significantly changes after the addition of P4VPBrD at degrees of quaternisation 45%. It is apparent also, from the impedance results shown in the Table 3, the value of R_t increase with increase in the concentration of P4VPBrD inhibitor and amelioration in the protection of the surface; this indicated an increase in the corrosion inhibition efficiency. The decrease in C_{dl} may be due to the adsorption of this compound on the metal surface leading to the formation of film from acidic solution [14, 37, 48, 49].

Table 3. EIS data of iron in 1M H₂SO₄ for various concentrations of P4VPBrD at degrees of quaternisation 45%.

Concentration (M)	R _t (Ω.cm ²)	f _o (Hz)	C _{dl} (μF/cm ²)	E%
Blank	17.5	100	91.2	---
10 ⁻⁸	23.1	43.29	64.6	24.3
10 ⁻⁷	52.5	42.02	59.2	66.7
510 ⁻⁷	126.2	40.2	74.1	86.1
10 ⁻⁶	173.8	36.12	58.2	89.9
510 ⁻⁶	489.8	35.45	48.2	96.4
10 ⁻⁵	589.8	25.28	38.1	97.0

The size of capacitive loop significantly decreased with the further increase of concentration of P4VPBrD at degrees of quaternisation 45%. The former shows that the mass transport has high

influence on the corrosion reaction after 30mn of immersion, whereas latter indicates that the corrosion resistance is increasing.

Generally, the pure sulphuric acid and sulphuric acid solution-containing P4VPBrD at degrees of quaternisation 45% used in our experiments were all desaerated. Dissolved oxygen may be reduced on iron surface and this will enable some corrosion to take place [27].

Electrochemical Impedance Spectroscopy (EIS) is a very powerful tool for the analysis of complex electrochemical systems. This Note is a practical discussion of the most common method for EIS data analysis. We measured an electrochemical cell’s complex impedance over a wide range of AC frequencies. Typically, several cell elements and cell characteristics contribute to the system’s EIS spectrum. The most common method used to analyze EIS spectra is equivalent circuit modelling in our case was modelled using the zview2.8d software after converting data from Radiometer Analytical EIS file converter. We simulate the cell incorporating the elements mentioned above. The behaviour of each element is then described in terms of “classical” electrical components R, C and L with the effects resistive, capacitive and inductive respectively.

The first step in the process is an educated guess. We predict the system elements that we feel will play a part in the cell’s impedance. We then build these elements into an Equivalent Circuit Model. The arrangement of the elements into logical series and parallel combinations is critical to the success of the modelling effort. Each element in the model has known impedance behaviour. The impedance of the element depends on the element type and the value(s) of the parameter(s) that characterize that element [50-53].

This model represents one possible assignment of the circuit elements to physical phenomena in the film on a metal surface. EIS data for electrochemical are most often represented in Nyquist plots as shown in Figure.3. It seems natural to make the analogy between electrical impedance and electrochemical impedance. These models are then used to adjust the experimental patterns to extract the parameters needed to understand the system studied. The most common model is the model proposed [22, 54]. It is presented in Figure 4 .

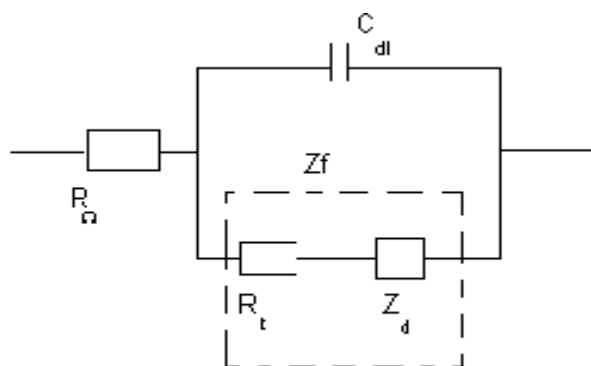
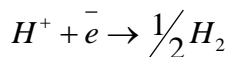


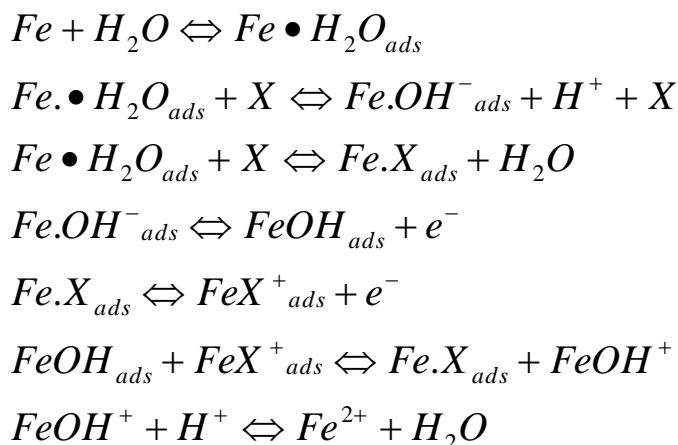
Figure 4. Equivalent circuit modelling of EIS for P4VPBrD at degree of quaternisation 45% at various concentrations

Theoretically, pure iron can hardly be corroded in the deoxygenated dilute sulphuric acid [28], as iron can displace hydrogen from acid solutions according to theories of chemical thermodynamic. It is a good approximation to consider the hydrogen evolution reaction and only consider oxygen reduction in the des-aerated sulphuric acid solutions at corrosion potential.

Cathodic reduction of hydrogen can be expressed either by a direct two electron transfer as shown by following Equation.



Dissolution of iron in sulphuric acid is described by the following equations. This behaviour can be explained by considering the mechanism of iron oxidation in acidic solution proceeding via one adsorbed intermediate, while in the presence of inhibitor a different mechanism has to be developed, involving to adsorbed intermediates. It is commonly accepted that the kinetics of iron anodic oxidation in acid depends on the adsorbed intermediate $FeOH_{ads}$ [27,29]. An iron anodic oxidation mechanism, which is valid in the presence of inhibitor, could be one similar to that discussed by Hackerman [27,30].



The species X is the inhibitor molecule, in our case. This mechanism shows that the anodic reaction kinetics is affected by two intermediates: one involving adsorbed hydroxyl ($FeOH_{ads}$) and the other involving the adsorbed inhibitor molecule (FeX_{ads}). The rate of anodic dissolution (step 4) depends to the product of step 2, but the two competitive steps 2 and 3 are based on the $Fe.H_2O_{ads}$. Displacements of the adsorbed water molecule by the species X, can affect the step 4. Every condition, such as molecular shape or localized partial charges or by another view, strict hindrance of X molecule to the metal surface, can variegate the above competition.

We note again, the inhibitory efficiency is independent of quaternisation degree of P4VPBrD. These results are in good agreement with the study of the action of a poly (4-vinylpyridine poly-3-oxide ethylene) in two degree of quaternisation 20% and 80% in corrosion of iron in molar sulphuric acid [32] and poly (4-vinylpyridine isopentyl bromide) (P4VPIPr) in three degrees of quaternisation (6%, 18% and 79 %).

3.4. Adsorption isotherm.

Several adsorption isotherms were assessed and the Langmuir adsorption isotherm was found to be the best description of the adsorption behaviour of the studied inhibitor, which obeys to:

$$\frac{C_{\text{inh}}}{\theta} = \frac{1}{b} + C_{\text{inh}} \quad (6)$$

$$b = \frac{1}{55,5} \cdot \exp\left(-\frac{\Delta G^{\circ}_{\text{ads}}}{R.T}\right) \quad (7)$$

C_{inh} is the inhibitor concentration; θ is the fraction of the surface covered, b is the adsorption coefficient and $\Delta G^{\circ}_{\text{ads}}$ is standard free energy of adsorption.

The adsorption isotherm can be determined if the inhibitor effect is due mainly to the adsorption on the metal surface (i.e, to its blocking). The type of the adsorption isotherms provides information about the interaction among the adsorbed molecules themselves and also their interactions with the electrode surface. Figure 5 show the dependence of the ration of the surface covered C/θ as function of the concentration (C) of P4VPBrD at degrees of quaternisation 45%. The degree of surface coverage θ for different concentrations of the inhibition in acidic media has been evaluated from weight loss using the equation [28, 46]:

$$\theta = \frac{W_{(\theta=0)} - W_{\theta}}{W_{(\theta=0)} - W_{(\theta=1)}} \quad (8)$$

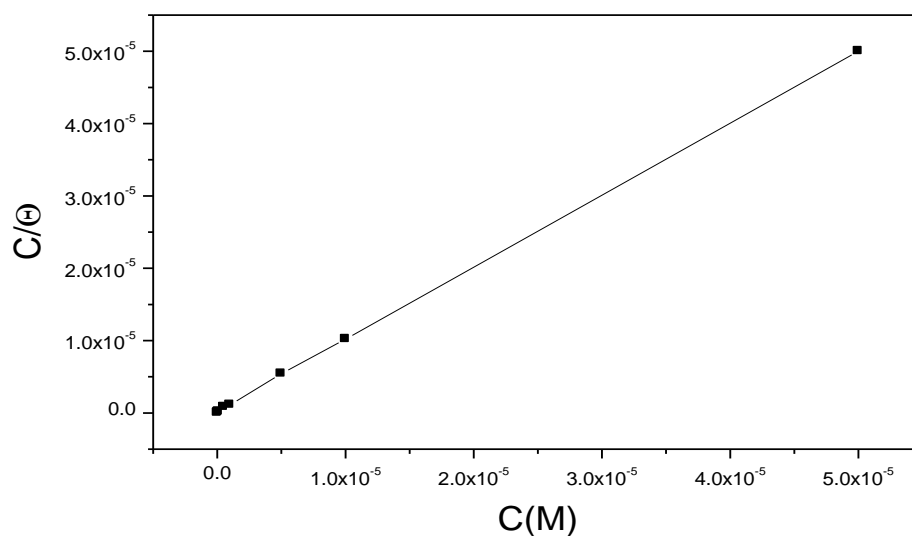
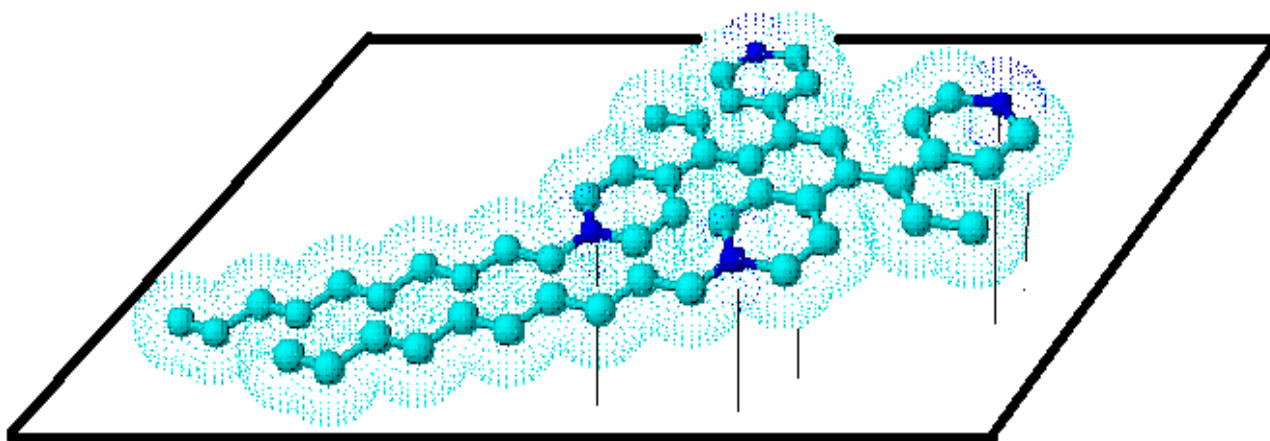


Figure 5. Langmuir isotherm adsorption model of P4VPBrD at degrees of quaternisation 45% on the surface of pure iron in 1M H₂SO₄.

Figure 5 illustrates the dependence of the fraction of the concentration and the surface covered C/θ as function of the concentration of the P4VPBrD at degrees of quaternisation 45%. The obtained plot of inhibitor is linear with a slope 0.99714 to close to unity. The regression coefficient is $R = 0.99996$ the intercept permit the calculation of the equilibrium constant b which is $5546311.702 \text{ M}^{-1}$ which leads to evaluate $\Delta G_{\text{ads}}^{\circ} = -48.40 \text{ kJ/mol}$. The large negative values of $\Delta G_{\text{ads}}^{\circ}$ ensure the spontaneity of the adsorption process and the stability of the adsorbed layer on the pure iron surface as well as a strong interaction between the P4VPBrD at degrees of quaternisation 45% molecules and the metal surface [34, 36, 49, 55], this value indicates also that inhibitor interacts on the pure iron surface by chemisorptions. This mode may be reinforced by the nature of mixed type inhibitory of the polymer by simultaneous action on both anodic and cathodic reactions. These results indicate that the presence of P4VPBrD at degrees of quaternisation 45% increases the inhibition efficiency without change in adsorption mechanism. The results suggest that the experimental data are well described by Langmuir isotherm.

The polymer is endowed besides centres nitrogenous strongly coordinate, which facilitate the adsorption to the surface of the metal. The adsorption of P4VPBrD at degrees of quaternisation 45% on the metal surface can occur either directly via donor-acceptor interactions between the π -electrons and free pair electrons of the heterocyclic compound and the vacant d-orbital's of surface iron atoms [19-22]. The polymer may be adsorbed on the metal surface in the form of neutral molecules involving the replacement of water molecules from the metal surface and sharing of electrons between the nitrogen atoms and the metal surface [31-34].



Scheme 2. Adsorption mode of P4VPBrD suggested on the iron surface.

It may result from the fact that adsorption amount and the coverage of the polymers on the electrode surface increases with increasing concentration. Thus, the electrode surface is efficiently separated from the medium. It is worth noting that, the presence of the inhibitor does not alter the profile of the impedance spectra, suggesting similar mechanisms for the metal dissolution in H_2SO_4 solution in the absence and presence of the inhibitor.

The high inhibition efficiency of P4VPBrD is attributed to the presence of additional electron donor atoms and N-heterocyclic, active centre of adsorption, which facilitates the strong binding of this compound to the surface. This can be explained by the forming of a protective coating under shape painting on the surface of the electrode shows in the scheme 2.

3.5. Effect of temperature.

Temperature can affect the iron corrosion in the acidic media in the absence and presence of inhibitor. To determine the action energy of the corrosion process, gravimetric measurements were taken at various temperatures (298K – 353K) in the absence and presence of P4VPBrD at degrees of quaternisation 45% at 5×10^{-5} M. The corresponding results are given in Table3.

Table 4. Effect of temperature in 1M H₂SO₄ and added of 5×10^{-5} M P4VPBrD (II).

T (K)	W (mg/ cm ² .h)	W' (mg/cm ² .h)	E (%)
298	2.448	0.000	100
308	4.018	0.000	100
318	8.034	0.243	97
328	17.88	0.726	96
338	22.48	1.124	95
353	59.45	3.567	94

The corresponding results given in Table (4) shows that the corrosion rate increases in the blank with the rise of temperature, but in the presence of the P4VPBrD at degrees of quaternisation 45% polymer a slight the dissolution of the pure iron is observed. The inhibitive efficiency of the polymer is seen to be almost constant with the rise of temperature indicating the nature of adsorption mechanism.

Although the weight-loss due to the corrosion increases with temperature, the inhibitive efficiency of P4VPBrD at degrees of quaternisation 45% was found to increase slightly with rise in temperature from 298K to 353K. Such inhibitor had a practical interest where retardation of corrosion at elevated temperature is desired, for example in pickling process.

Figure 6 shows Arrhenius plots for iron corrosion. The apparent activation energies can be determined by the relation where E_a and E'_a are the apparent activation corrosion energies in the absence and presence of P4VPBrD, respectively:

$$\begin{aligned}
 W' &= K \exp\left(\frac{-E'_a}{RT}\right) \\
 W &= K \exp\left(\frac{-E_a}{RT}\right)
 \end{aligned}
 \tag{9}$$

$E_a = 22.18 \text{ kJ.mol}^{-1}$ and $E_a' = 30.01 \text{ kJ.mol}^{-1}$ are the apparent activation energies in the presence and absence of P4VPBrD at degrees of quaternisation 45%, respectively. We notice that the apparent activation energy is almost the same in the presence and absence of inhibitor. The 7.83 kJ.mol^{-1} increase in the apparent activation energy may be interpreted as physical adsorption that occurs in the first stage.

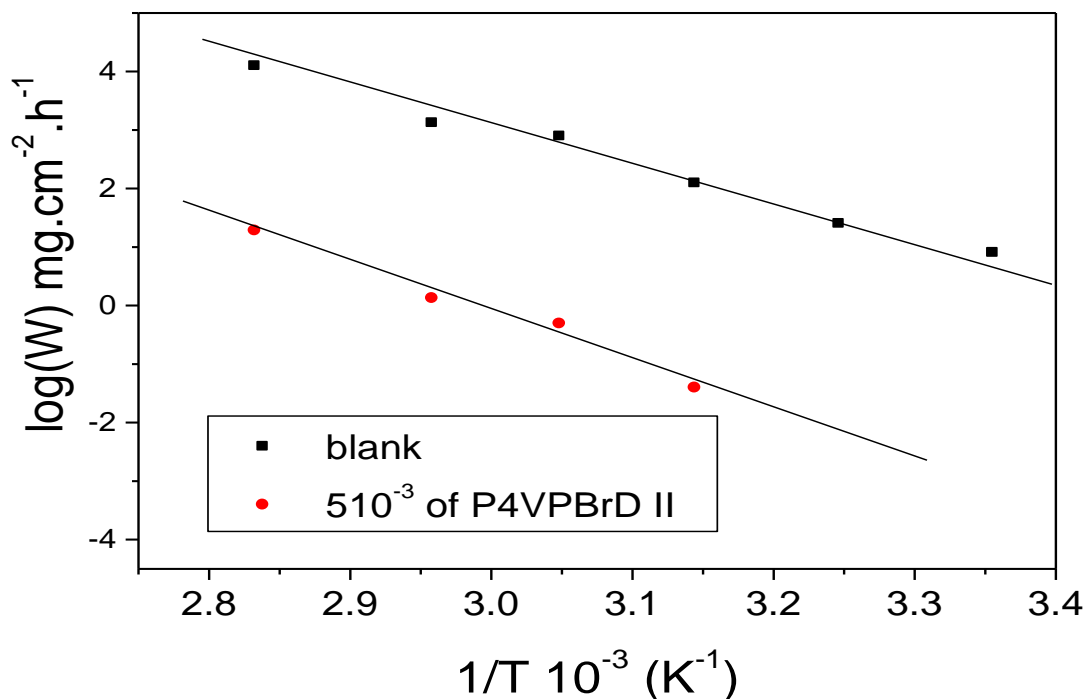


Figure 6. Arrhenius straight lines for P4VPBrD at degrees of quaternisation 45%.

The increase in activation energy can be stated as to an appreciable decrease in the adsorption of the inhibitor on the iron pure surface with increase in temperature. The slight increase of E_a did not exclude the physical interaction between the inhibitor and metal surface. Near these findings, we may introduce that the polymer adsorbed on the iron surface by the two modes: chemical and physical adsorption

4. CONCLUSION

The use of impedance measurements particularly for corrosion studies in extremely resistive medium in increasing. We verified:

- The type molecules have been low-cost and stable corrosion inhibitors.
- Their inhibition efficiency ($E\%$) increases with the concentration for all inhibitors and attains around 98 % at 10^{-5} M .
- The inhibitory efficiency is independent of quaternisation degree of P4VPBrD at tree degree of quaternisation 25%, 45% and 60% and was found to increase slightly with rise in temperature from 298 to 353 K.

- Steady state electrochemical and gravimetric measurements have shown that the polymer acts predominantly as a mixed inhibitor for the corrosion of iron in 1M H₂SO₄ without modifying the mechanism of hydrogen evolution reaction.
- The polarisation resistance of the system increases when the polymer is added to the solution.
- The decrease in C_{dl} may be due to the adsorption of these compounds on the metal surface leading to the formation of film from acidic solution and Nyquist diagrams of P4VPBrD at tree degree of quaternisation 25%, 45% and 60% present a semicircle. It shows that a charge transfer process mainly controls the corrosion of iron.

ACKNOWLEDGEMENTS

Prof S. S. Al-Deyab and Prof B. Hammouti extend their appreciation to the Deanship of Scientific Research at king Saud University for funding the work through the research group project 089.

References

1. S. Kim, J. Surek, J. Baker-Jarvis, *Journal of Research of the National Institute of Standards and Technology*, 116 (2011) 655.
2. H.Y. Du, Y.H. Wei, W.M. Lin, L.F. Hou, Z.Q. Liu, Y.L. An, W.F. Yang, *App. Surf. Sci.*, 255 (2009) 8660.
3. G. Gece, S. Bilgic, *Corr. Sci.*, 52 (2010) 3435.
4. K. Tebbji, A. Aouniti, A. Attayibat, B. Hammouti, H. Oudda, M. Benkaddour, S. Radi, A. Nahle, *Indian J. Chem. Technol.*, 18 (2011) 244.
5. K. Tebbji, H. Oudda, B. Hammouti, M. Benkaddour, S.S. Al-Deyab, A. Aouniti, S. Radi, A. Ramdani, *Research on Chemical Intermediates*, 37 (2011) 985.
6. S.Y. Wei, P. Mavinakuli, Q. Wang, D. Chen, R. Asapu, Y.B. Mao, N. Haldolaarachchige, D.P. Young, Z.H. Guo, *J. Electrochem. Soc.*, 158 (2011) K205.
7. A. Zarrouk, B. Hammouti, R. Touzani, S.S. Al-Deyab, M. Zertoubi, A. Dafali, S. Elkadiri, *Int. J. Electrochem. Sci.*, 6 (2011) 4939.
8. A. Zarrouk, B. Hammouti, H. Zarrok, S.S. Al-Deyab, M. Messali, *Int. J. Electrochem. Sci.*, 6 (2011) 6261.
9. J.H. Zhu, S.Y. Wei, Y.F. Li, S. Pallavkar, H.F. Lin, N. Haldolaarachchige, Z.P. Luo, D.P. Young, Z.H. Guo, *J. Mater. Chem.*, 21 (2011) 16239.
10. M. Benabdellah, K.F. Khaled, B. Hammouti, *Materials Chemistry and Physics*, 120 (2010) 61.
11. F.Z. Bouanis, C. Jama, M. Traisnel, F. Bentiss, *Corr. Sci.*, 52 (2010) 3180.
12. K. Bouhriha, F. Ouahiba, D. Zerouali, B. Hammouti, M. Zertoubi, N. Benchat, *E-Journal of Chemistry*, 7 (2010) S35.
13. M. Dahmani, A. Et-Touhami, S.S. Al-Deyab, B. Hammouti, A. Bouyanzer, *Int. J. Electrochem. Sci.*, 5 (2010) 1060.
14. M. Benabdellah, A. Tounsi, K.F. Khaled, B. Hammouti, *Arabian Journal of Chemistry*, 4 (2011) 17.
15. A. Chetouani, M. Daoudi, B. Hammouti, T. Ben Hadda, M. Benkaddour, *Corr. Sci.*, 48 (2006) 2987.
16. A. Chetouani, B. Hammouti, T. Benhadda, M. Daoudi, *App. Surf. Sci.*, 249 (2005) 375.
17. L. Afia, R. Salghi, L. Bammou, L. Bazzi, B. Hammouti, *Acta Metallurgica Sinica-English Letters*, 25 (2012) 10.

18. O.K. Abiola, M.O. John, P.O. Asekunowo, P.C. Okafor, O.O. James, *Green Chemistry Letters and Reviews*, 4 (2011) 273.
19. L. Afia, R. Salghi, E. Bazzi, L. Bazzi, M. Errami, O. Jbara, S.S. Al-Deyab, B. Hammouti, *Int. J. Electrochem. Sci.*, 6 (2011) 5918.
20. L. Bammou, M. Mihit, R. Salghi, A. Bouyanzer, S.S. Al-Deyab, L. Bazzi, B. Hammouti, *Int. J. Electrochem. Sci.*, 6 (2011) 1454.
21. M. Behpour, S.M. Ghoreishi, N. Mohammadi, M. Salavati-Niasari, *Corr. Sci.*, 53 (2011) 3380.
22. F. Bentiss, C. Jama, B. Mernari, H. El Attari, L. El Kadi, M. Lebrini, M. Traisnel, M. Lagrenee, *Corr. Sci.*, 51 (2009) 1628.
23. M. Znini, L. Majidi, A. Laghchimi, J. Paolini, B. Hammouti, J. Costa, A. Bouyanzer, S.S. Al-Deyab, *Int. J. Electrochem. Sci.*, 6 (2011) 5940.
24. S. Kertit, F. Chaouket, A. Srhiri, M. Keddou, *Journal of Applied Electrochemistry*, 24 (1994) 1139.
25. N. Kouloumbi, G.M. Tsangaris, S.T. Kyvelidis, *Journal of Coatings Technology*, 66 (1994) 83.
26. S. Kertit, J. Aride, A. Srhiri, A. Benbachir, K. Elkacemi, M. Etman, *Journal of Applied Electrochemistry*, 23 (1993) 835.
27. C. Chetouani, K. Medjahed, K.E. Sid-Lakhdar, B. Hammouti, M. Benkaddour, A. Mansri, *Corr. Sci.*, 46 (2004) 2421.
28. A. Chetouani, K. Medjahed, K.E. Benabadji, B. Hammouti, S. Kertit, A. Mansri, *Progress in Organic Coatings*, 46 (2003) 312.
29. H. Dolas, A.S. Sarac, *J. Electrochem. Soc.*, 159 (2012) D1.
30. R.S. Hastak, P. Sivaraman, D.D. Potphode, K. Shashidhara, A.B. Samui, *Electrochimica Acta*, 59 (2012) 296.
31. R.L. Lavall, S. Ferrari, C. Tomasi, M. Marzantowicz, E. Quartarone, M. Fagnoni, P. Mustarelli, M.L. Saladino, *Electrochimica Acta*, 60 (2012) 359.
32. H. Bhandari, V. Choudhary, S.K. Dhawan, *Synthetic Metals*, 161 (2011) 753.
33. Y. Abed, Z. Arrar, A. Aouiniti, B. Hammouti, S. Kertit, A. Mansri, *J. Chim. Phys.* 96 (1999) 1347.
34. Y. Abed, B. Hammouti, F. Touhami, A. Aouiniti, S. Kertit, A. Mansri, K. Elkacemi, *Bull. Electrochem.* 17 (2001) 105.
35. Y. Abed, Z. Arrar, B. Hammouti, M. Taleb, S. Kertit, A. Mansri, *Anti-corros. Met and Mater.* 48 (2001) 304.
36. A. Ouchrif, M. Zegmout, B. Hammouti, A. Dafali, M. Benkaddour, A. Ramdani, S. Elkadiri, *Progress in Organic Coatings*, 53 (2005) 292.
37. M. Bouklah, H. Harek, R. Touzani, B. Hammouti, Y. Harek, *Arabian Journal of Chemistry*, 5 (2012) 163.
38. M. Benabdellah, A. Yahyi, A. Dafali, A. Aouiniti, B. Hammouti, A. Ettouhami, *Arabian Journal of Chemistry*, 4 (2011) 243.
39. G. Thomas, N. Hammouti, A. Seitz, *Journal of Shellfish Research*, 30 (2011) 123.
40. O. Senhaji, R. Taouil, M.K. Skalli, M. Bouachrine, B. Hammouti, M. Hamidi, S.S. Al-Deyab, *Int. J. Electrochem. Sci.*, 6 (2011) 6290.
41. L. Herrag, B. Hammouti, S. Elkadiri, A. Aouiniti, C. Jama, H. Vezin, F. Bentiss, *Corrosion Science*, 52 (2010) 3042.
42. M. Lebrini, M. Traisnel, M. Lagrenee, B. Mernari, F. Bentiss, *Corr. Sci.*, 50 (2008) 473.
43. F. Bentiss, M. Lagrenee, M. Traisnel, B. Mernari, H. Elattari, *J. App. Electrochem.*, 29 (1999) 1073.
44. B. Mernari, H. El Attari, M. Traisnel, F. Bentiss, M. Lagrenee, *Corr. Sci.*, 40 (1998) 391.
45. Y. Oyama, A. Nishikata, T. Tsuru, *Journal of the Japan Institute of Metals*, 66 (2002) 690.
46. A. Chetouani, B. Hammouti, A. Aouiniti, N. Benchat, T. Benhadda, *Progress in Organic Coatings*, 45 (2002) 373.

47. A. Chetouani, A. Aouniti, B. Hammouti, N. Benchat, T. Benhadda, S. Kertit, *Corrosion Science*, 45 (2003) 1675.
48. M. Znini, M. Bouklah, L. Majidi, S. Kharchouf, A. Aouniti, A. Bouyanzer, B. Hammouti, J. Costa, S.S. Al-Dyab, *Int. J. Electrochem. Sci.*, 6 (2011) 691.
49. M. Bouklah, A. Attayibat, S. Kertit, A. Ramdani, B. Hammouti, *App. Surf. Sci.*, 242 (2005) 399.
50. J. Gomez, R. Nelson, E.E. Kalu, M.H. Weatherspoon, J.P. Zheng, *Journal of Power Sources*, 196 (2011) 4826.
51. N. Hannachi, K. Guidara, F. Hlel, *Ionics*, 17 (2011) 463.
52. D.A. Harrington, P. van den Driessche, *Electrochimica Acta*, 56 (2011) 8005.
53. N.H. Helal, W.A. Badawy, *Electrochimica Acta*, 56 (2011) 6581.
54. V.V. Nikonenko, A.E. Kozmai, *Electrochimica Acta*, 56 (2011) 1262.
55. S. Kertit, B. Hammouti, *App. Surf. Sci.*, 93 (1996) 59